NANO LETTERS

2007
Vol. 7, No. 12
3576−3582

Mesoporous Silica Particles Induce Size Dependent Effects on Human Dendritic Cells

Helen Vallhov,*,† Susanne Gabrielsson,† Maria Strømme,‡ Annika Scheynius,† and Alfonso E. Garcia-Bennett‡

Clinical Allergy Research Unit, Department of Medicine Solna, L2:04, Karolinska Institutet and University Hospital, Solna, 171 76 Stockholm, Sweden, and Nanotechnology and Functional Materials, Department of Engineering Sciences, The Ångström Laboratory, Uppsala University, Box 534, 751 21 Uppsala, Sweden

Received June 21, 2007; Revised Manuscript Received October 11, 2007

ABSTRACT

The effects of mesoporous silica nano- (270 nm) and microparticles (2.5 μm) with surface areas above 500 m²/g were evaluated on human monocyte-derived dendritic cells (MDDC). Size- and concentration-dependent effects were seen where the smaller particles and lower concentrations affected MDDC to a minor degree compared to the larger particles and higher concentrations, both in terms of viability, uptake, and immune regulatory markers. Our findings support the further development of mesoporous silica particles in drug and vaccine delivery systems.

Nanoporous materials such as mesoporous silicates are being utilized in a variety of biorelated applications as a result of their high specific surface areas, internal pore volumes, tailorable surfaces, and high chemical and thermal stabilities. First discovered in 1992,[1] the material properties promise many advantages in several important applications including their use as catalysts and catalyst supports, adsorbents, sensors, in separation and purification technologies, and as insulators.[2,3] In life sciences, mesoporous materials may offer advantages over current adjuvants in drug delivery systems, tissue engineering, labeling and bioseparation material technologies, and transfection devices.[4]

Of the many nanoporous materials available, covering a pore size spectrum ranging from 0.5 to 500 nm, those in the mesoscale (2−50 nm) are of particular interest in biotechnologies because a large proportion of biomolecules are within this size range. Hence, the adsorption of active pharmaceutical molecules into stabile, nonerosive mesoporous materials has been explored offering the potential to control (delay) drug release, enhance drug dissolution, promote drug permeation across the intestinal cell wall, and improve drug stability under the extreme environment of the gastro-intestinal tract when administered orally.[5] Different types of drug molecules (including macromolecules) can be adsorbed into mesoporous micro- and nanoparticles by modifying the pore architecture and surface chemistry of the carrier material.[6] Recently Lin et al., have reported a novel gene transfection device based on polyamidoamine (PAMAM) dendrimers supported on mesoporous materials. In this work, plasmid DNA (pEGFP-C1 vector) was electrostatically attached to the surface of a mesoporous material via the PAMAM polymer. Gene transfection efficacy and biocompatibility of the mesoporous particles were derived with neural glia (astrocytes), human cervical cancer (HeLa) cells, and chinese hamster ovarian (CHO) cells showing transfection enhancement that was attributed to a particle sedimentation effect.[7]

Some initial work has been conducted to identify toxicological behavior effects of silica materials, but this is mainly based on crystalline zeolites or on bioactive glass.[8,9] The fundamental differences in comparison to the zeolites and bioactive glasses, the use of these solids in nanoparticle powdered form, and their introduction into the medical field warrant an in depth study of the possible hazardous or immunomodulatory effects. Because the physiochemical properties of nanomaterials are different from those of their bulk counterparts, their interaction with biological systems is expected to be different. The effects may vary between different kinds of nanoparticles, depending, for instance, on chemical composition, crystallinity, size, shape and surface area.[10] Mesoporous materials offer extremely high surface areas, even above 1000 m²/g, and are typically composed of monodispersed particles with amorphous silica walls.[1−3]

* Corresponding author. E-mail: helen.vallhov@ki.se.
† Karolinska Institutet and University Hospital.
‡ Uppsala University.

10.1021/nl0714785 CCC: $37.00
Published on Web 11/02/2007

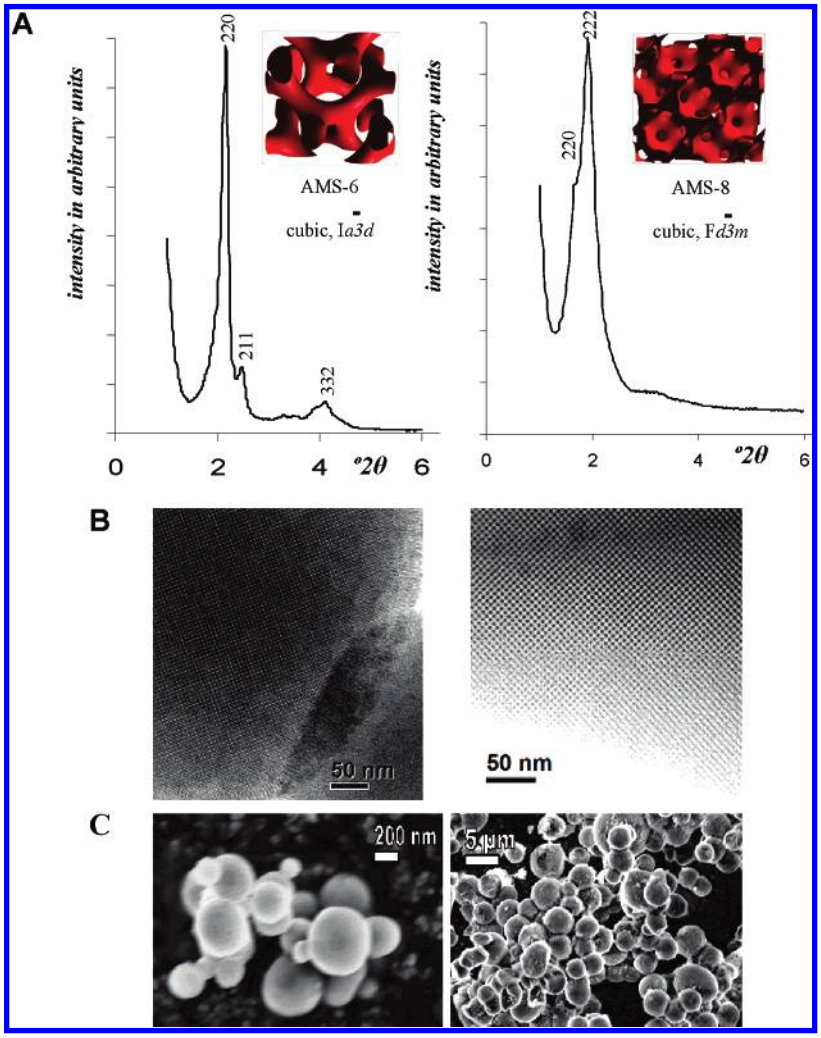

Figure 1. Structural and textural characterization of mesoporous materials prepared. (A) Powder XRD data showing mesoscale peaks consistent with cubic mesoporous structures, AMS-6 (left) and AMS-8 (right). Insets show comparison and schematic representations of the pore/cage connectivities for the two structures showing the arrangement of cylindrical pores in AMS-6 and of cage-type pores in bimodal AMS-8. (B) Representative TEM images recorded on calcined samples of AMS-6 (left) and AMS-8 (right) structures. Both images are taken along the [100] directions. (C) SEMi images showing the representative morphologies of AMS-6 (left) and AMS-8 (right). Average particle size calculated from SEMi and TEM observation were 270 nm and 2.5 μm for AMS-6 and AMS-8, respectively.

Human antigen presenting dendritic cells (DC) have been described as the sentinels of the immune system, and they have an exceptional capacity to initiate both primary and secondary immune responses in vivo.[11] By expressing costimulatory molecules such as CD40, CD80, CD86, and peptides loaded onto major histocompatibility complex (MHC) class I and II and by production of cytokines like IL-10 or IL-12, they interact with lymphocytes of the T cytotoxic or T helper (Th) phenotype. The latter then may differentiate into discrete subsets of cytokine-secreting cells such as those represented by the Th1, Th2, or T-regulatory type of T-lymphocytes.[12] Th1 cells, which stimulate eradication of intracellular pathogens, are characterized by their production of IFN-γ and potentiates cell-mediated immunity. Th2 cells, which evolved to enhance elimination of parasitic infections, are characterized by production of IL-4, IL-5, and IL-13, which are potent activators of antibody production and have a central role in allergic diseases.[13] To regulate these potentially dangerous immune responses, DC also can stimulate expansion of antigen-specific regulatory T cells that are able to produce IL-10 or TGF-β.[14] Particles with the capacity to induce specific changes in DC phenotype and thus also in T lymphocyte induction and balance are attractive immunotherapeutic tools because immune responses could theoretically be tailor-made depending on the desired effect.

Our primary goal here was to determine the effect of mesoporous particles of different sizes and structures on DC. For this purpose, we have chosen the mesostructures AMS-6 and AMS-8, which have been shown to possess three-dimensional cubic cylindrical and cubic cage type pore geometries, respectively.[15] We have used *N*-lauroyl-amino acid anionic surfactants in combination with alkoxysilanes for the co-operative self-assembly of micelles and silica species (see Supporting Information for specific preparation details). The structural and textural characterizations of AMS-6 and AMS-8 are shown in Figure 1. Powder X-ray diffractograms (XRD) (Figure 1A) show mesoscale peaks consistent with the formation of cubic mesostructures. Transmission electron microscopy (TEM) analysis on surfactant removed (calcined) samples (Figure 1B) allowed the

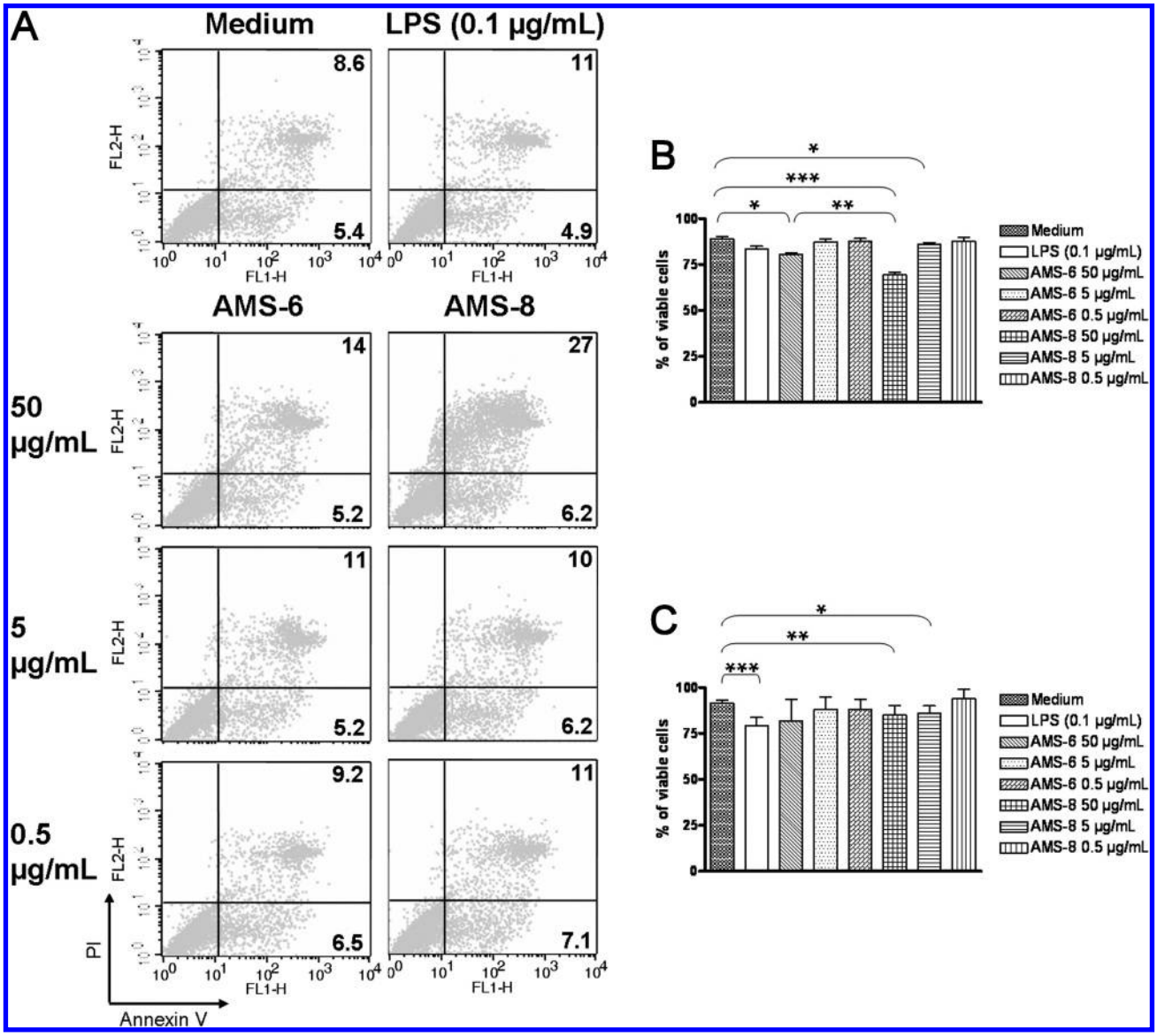

Figure 2. The viability of MDDC was decreased by AMS-6 and AMS-8 at 24 h. (A) PI and Annexin-V staining was used to analyze the viability of MDDC after co-culturing with silica particles. The percentages of stained/unstained cells are shown in each quadrant. The results shown are from one representative experiment of four using MDDC generated from different blood donors. (B) The total sum of necrotic, early, and late apoptotic cells at 24 h using PI and Annexin-V staining was quantified. Results represent the mean ± SEM from four independent experiments. (C) Trypan-blue staining was used as a complementary viability method at 24 h. Results represent the mean ± SEM from six independent experiments using cells from different healthy blood donors. MDDC cultured in medium only was included as a negative control and LPS was included as a positive control (0.1 μg/mL) in both methods. * $P < 0.05$, ** $P < 0.01$, *** $P < 0.001$.

confirmation of the two mesoporous structures of AMS-6 and AMS-8, where contrast patterns and Fourier transform diffractograms (not shown) are typical of these systems.[16] The unit cell parameters for calcined samples, as derived from the XRD patterns, were 100.5 and 158.8 Å for AMS-6 and AMS-8, respectively, and are consistent with previously published data.[17] Scanning electron microscopy (SEMi) images recorded on calcined samples showed particle sizes of 270 nm (±50 nm) for AMS-6 and of 2.5 μm (±500 nm) for AMS-8 (Figure 1C). To increase the monodisperity, powders were sonicated (65 W for 10 min, Sonic Vibracell) prior to use. Pore size distribution curves obtained from nitrogen adsorption−desorption isotherms performed on calcined samples were centered at 3.9 and 2.8 nm for AMS-6 and AMS-8, respectively. Mesoporous surface areas were calculated using the BET method (Brunauer−Emmett−Teller)[18] as 520 m^2/g (calcined AMS-6) and 547 m^2/g (calcined AMS-8), thus almost being similar. Possible bacterial lipopolysaccharide (LPS) contaminants were analyzed with the Limulus amebocyte lysate endochrome assay (Charles River Endosafe, Charleston, SC). The levels were always below 0.08 ng/mL. Because these preparations were further diluted in cell cultures, the final LPS concentrations were always lower than 2 pg/mL, shown to not have any effect on DC by itself.[19]

Human peripheral blood mononuclear cells from healthy blood donors were separated from buffy coats by standard gradient centrifugation (see Supporting Information). Monocyte derived DC (MDDC) were generated in the presence of IL-4 and GM-CSF as previously described.[20] At day 6 of

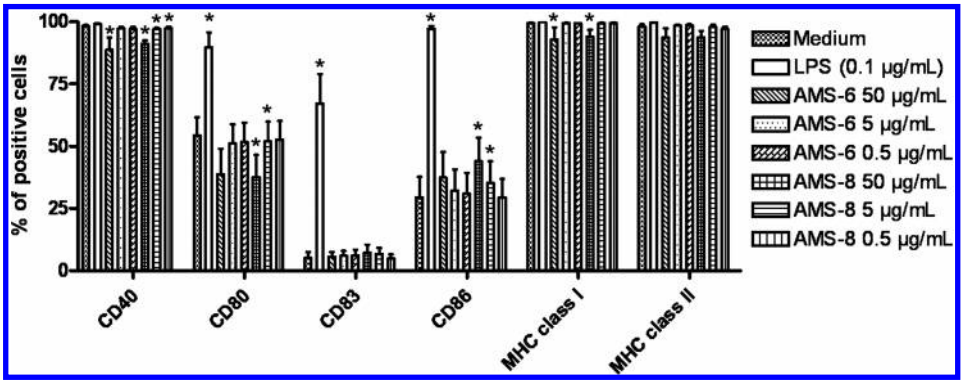

Figure 3. The mesoporous silica particles induce a size and concentration dependent immune regulatory effect. Expression of the co-stimulatory molecules CD40, CD80, CD86, and the maturation marker CD83 and the antigen presenting molecules MHC class I and II were analyzed by flow cytometry after 24 h and are presented as percentage of positive cells. For each sample, 10^4 cells within the gate for viable MDDC were analyzed. LPS (0.1 μg/mL) was used as a positive control. Results represent the mean ± SEM from six independent experiments using cells from different healthy blood donors. * $P < 0.05$, compared to MDDC cultured in medium alone.

culture, the immature MDDC were co-cultured with AMS-6 and AMS-8 (0.5, 5, or 50 μg/mL) for either 24 or 48 h. As controls, MDDC cultured in medium alone and cells treated with LPS (0.1 μg/mL; L8274, *Escherichia coli*, serotype 026-B6, Sigma-Aldrich, Steinheim, Germany) were used. The degree of apoptosis (programmed cell death) and necrosis was examined by measuring the binding of Annexin V-fluorescein and inclusion/exclusion of propidium iodide (PI) using a FACSCalibur flow cytometer. PI^-/Annexin V^+ events define early apoptosis and PI^+/Annexin V^+ are classified as late apoptosis or secondary necrosis (Figure 2A).[21] After summarizing the data for apoptotic and necrotic cells, a significant decrease in viability from 89 ± 1.1 in the medium control to 81 ± 0.8 and to 69 ± 1.3% was detected for the MDDC treated with the highest concentration of AMS-6 and AMS-8 for 24 h, respectively ($P < 0.05$ and $P < 0.001$, respectively, $n = 4$; Figure 2B). A significant difference in viability was also observed between the MDDC samples co-cultured with either AMS-6 or AMS-8, 50 μg/mL ($P < 0.01$, $n = 4$; Figure 2B). At a lower concentration of AMS-8 (5 μg/mL) a moderate albeit significant decrease in viability was seen ($P < 0.05$, $n = 4$; Figure 2B). After 48 h, only the highest concentration of AMS-8 induced a significant decrease in viability to 72 ± 4.3% compared to the medium control 85 ± 2.9% ($P < 0.01$, $n = 4$) and compared to AMS-6 at similar concentration (82 ± 2.7% viability, $P < 0.05$, $n = 4$; data not shown). The decreased viability involved mainly late apoptosis (PI^+/Annexin V^+; Figure 2A). To note, the silica particles themselves did also absorb PI, which needed to be taken into consideration while analyzing the toxicity results. Therefore, we also employed trypan blue exclusion as a complimentary method to study cell viability, and these findings supported our conclusions, except that there were no significant effects seen for AMS-6 compared to the medium control. Instead, a significant decrease in viability of the LPS treated MDDC ($P < 0.001$, $n = 6$) was observed at 24 h (Figure 2C), which is in accordance with a previous report for various other cell types.[22]

To investigate if the particles had any immune stimulatory or modulatory effects on MDDC, we performed flow cytometric analysis after co-culture for 24 and 48 h. AMS-8, at 50 and 5 μg per mL, induced at 24 h a significant increase of $CD86^+$ cells ($P < 0.05$, $n = 6$) and, interestingly, a corresponding significant decrease of $CD80^+$ cells ($P < 0.05$, $n = 6$) and $CD40^+$ cells ($P < 0.05$; $n = 6$) compared to MDDC cultured in medium alone (Figure 3). For AMS-6, a significant effect was only seen for CD40, which expression was reduced at the highest concentration of nanoparticles ($P < 0.05$, $n = 6$, Figure 3). Both AMS-6 and AMS-8 induced a slight decrease of MHC class I from 100 ± 0.13 to 93 ± 4.9 or to 92 ± 2.8%, respectively, compared to the medium control but only at the highest concentration used, 50 μg/mL ($P < 0.05$, $n = 6$ for both particles; Figure 3). After 48 h exposure with silica particles, the same pattern for all co-stimulatory and MHC molecules was observed (data not shown). There was no significant effect on the DC maturation marker CD83, nor on MHC class II at both time points (Figure 3 and data not shown). Thus, the data suggest a size and concentration dependent effect on the co-stimulatory molecules CD40, CD80, and CD86, although the cells remain in a relative immature state after incubation with the nano- and microparticles as compared to those cultured with LPS, which induced the expected maturation of the MDDC[19,23] (Figure 3).

The effects of both silica materials were further investigated by measuring the production of cytokines by MDDC. Thus, supernatants from MDDC cultured with silica particles were collected after 24 and 48 h, followed by analysis with ELISA. As expected,[24] LPS induced a significantly increased production of both IL-10 and IL-12p70 at both time points (data not shown and Figure 4). No detectable levels of IL-12 were seen at 24 h after stimulation with the mesoporous silica particles; however, at 48 h we saw increased levels compared to the medium control. This was mostly pronounced for AMS-8 at 50 μg/mL (Figure 4). IL-10 production was not detected in the cultures with the silica particles (data not shown).

The induced production of IL-12p70 but not of IL-10 and the enhanced expression of CD86 and the decreased numbers of $CD80^+$ and $CD40^+$ MDDC, especially seen after exposure to AMS-8 at the higher concentrations, suggests the induction

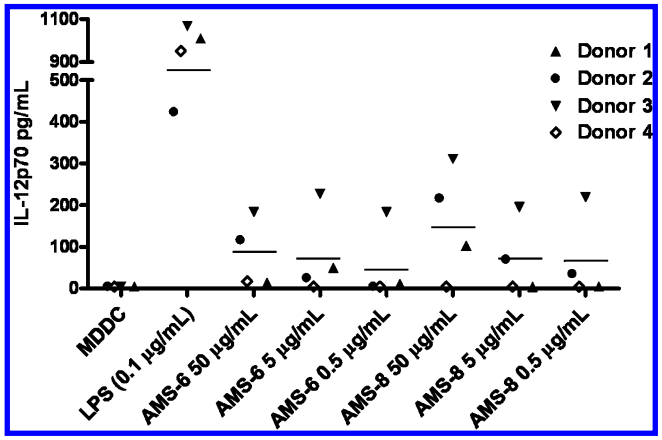

Figure 4. AMS-6 and AMS-8 induce production of IL-12p70. Concentrations in supernatants from MDDC cultured with mesoporous silica particles at a concentration of 50, 5, and 0.5 μg/mL for 48 h were analyzed for IL-12p70 with ELISA. MDDC cultured in medium only was included as a negative control and LPS (0.1 μg/mL) as a positive control. Results shown are from four independent experiments using cells from different healthy blood donors. The horizontal lines indicate the mean values.

of specific immune regulatory signals by these mesoporous particles. CD86 has been suggested to be involved in triggering naïve T-cells to Th2-cells, while CD80 and CD40 are more involved in Th1 responses.[25,26] The fact that the maturation marker CD83 is unaffected excludes a general maturation effect. However, whether the effect seen here on CD80/CD86 indeed has an effect on the Th1/Th2 balance remains to be established.

To further explore the interaction between silica particles and DC, we investigated whether the particles are internalized by MDDC. Within 10−60 min, an uptake of AMS-6 (Figure 5A) and AMS-8 (Figure 5B) was seen by the majority of the MDDC, as studied by confocal microscopy using FITC-conjugated silica particles and MDDC labeled with PI and Alexa Fluor 546 via anti-HLA-DR antibodies. No nuclear uptake was observed for either particle size, suggesting a low risk for interference with nuclear function, such as reported for smaller silica nanoparticles.[27] To investigate if the uptake of mesoporous silica particles is an energy dependent process, MDDC were kept at 4 °C during co-culture with particles for 3 h. Neither AMS-6 (Figure 5C) nor AMS-8 (Figure 5D) were internalized during the time period, suggesting that an active mechanism, such as endocytosis, is involved in the cellular uptake seen at 37 °C (see Supporting Information for z-scans, Figure S2). The uptake of AMS-6 and AMS-8 was additionally linked to an increased percentage of $CD86^+$ MDDC, as seen by FACS (Figure 5E). More $CD86^+$ cells containing FITC-labeled silica particles were observed for AMS-8 than for AMS-6. This difference was observed both at 24 h, where AMS-8 had a mean of 22 ± 2.9% double positive cells compared to 6.2 ± 1.4% for AMS-6 ($n = 4$), and at 48 h where the means were 16 ± 1.5 and 5.9 ± 1.0%, respectively ($n = 4$), thus suggesting a size-dependent uptake resulting in different numbers of $CD86^+$ cells. Decreased numbers of FITC positive cells were seen after 24 h, which suggests the capability of MDDC to release the mesoporous silica

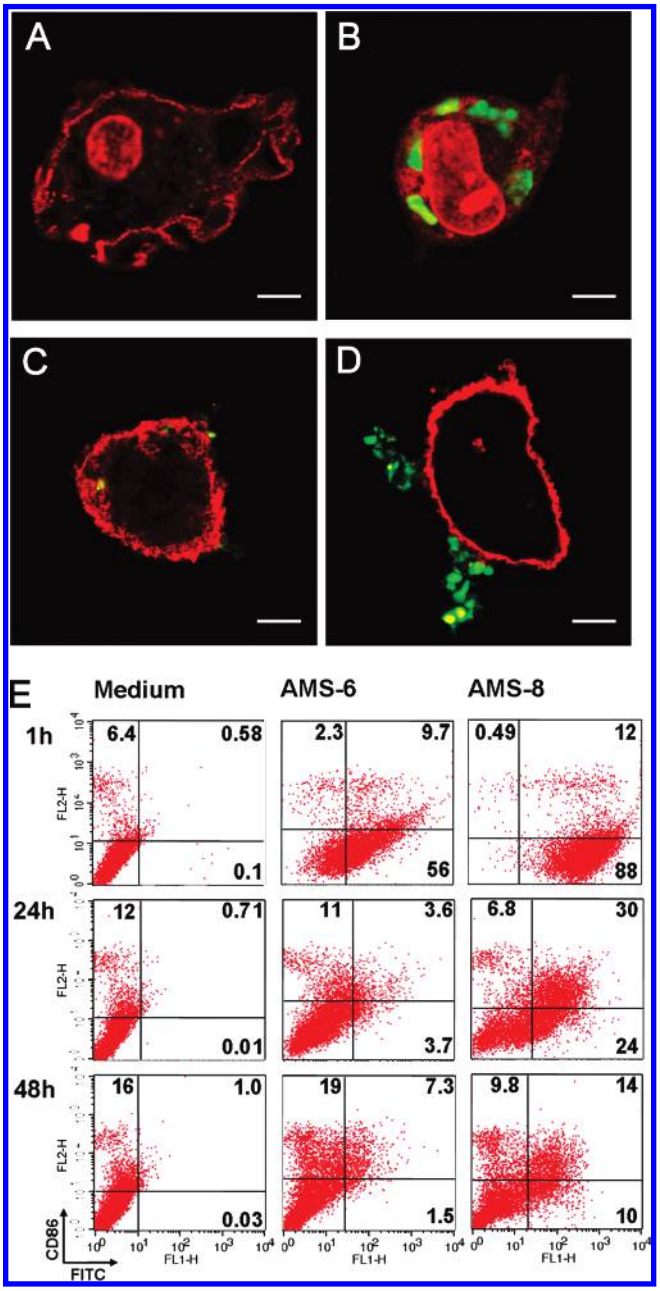

Figure 5. MDDC incubated with 50 μg of silica particles per mL show an active uptake of AMS-6 and AMS-8 combined with an increased expression of CD86. Confocal images (TCS SP2; Leica Microsystems, Mannheim, Germany) show a cellular but non-nuclear uptake of FITC-conjugated AMS-6 (A) and AMS-8 (B) after 1 h at 37 °C, while MDDC incubated with AMS-6 (C) and AMS-8 (D) for 3 h at 4 °C do not show this internalization. Scale bars represent 5 μm. (E) The uptake of FITC-conjugated particles at 37 °C was quantitatively studied by flow cytometry (FL1-H axis), which was linked to an increased expression of CD86 (FL2-H axis). The percentage of positive cells is shown in each quadrant. Results shown are representative of four independent experiments using MDDC generated from different healthy blood donors. 10^4 cells within the gate of viable cells were analyzed per sample.

particles after uptake. However, some of the MDDC may have contained too few FITC-labeled particles or some fading of the FITC fluorescence may have occurred with time, preventing the detection by FACS, which in turn could have had some effect on these results.

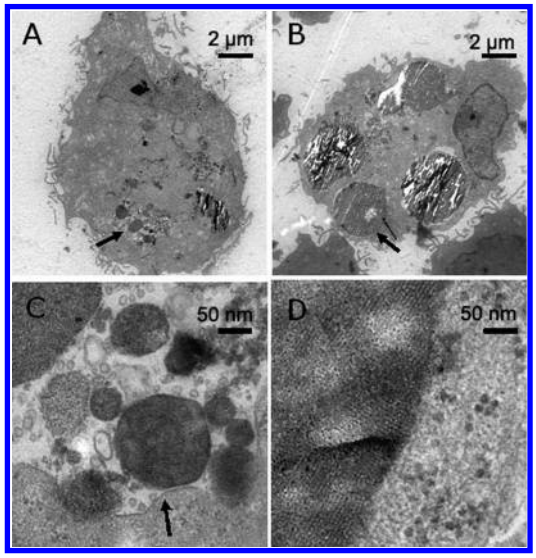

Figure 6. MDDC internalize unconjugated mesoporous silica particles at 37 °C. TEM for the unconjugated AMS-6 nano- (A) and AMS-8 microsized particles (B), shown here at 24 h. High-magnification TEM images recorded on AMS-6 (C) and AMS-8 (D) from areas highlighted by arrows. Arrow in (C) points to the vesicular membrane surrounding particles of AMS-6.

To further examine the localization of the particles inside the cell but also to exclude a FITC dependent internalization into MDDC, TEM was used as a complimentary method. TEM images supported our data, where an uptake was seen for both unconjugated AMS-6 (Figure 6A) and AMS-8 (Figure 6B). TEM data also showed that AMS-6 was encapsulated into vesicular compartments (Figure 6C), while around the larger spheres no membranelike structures could be detected (Figure 6D), suggesting a cytosolic localization. The absence of a membrane normally suggests a cellular passive uptake, but this is contradicted by the experiments performed at 4 °C. Therefore, an escape from the endolysosomal entrapment is suspected, which has been previously reported for mesoporous silica particles,[28] but this still remains to be investigated in our system. In general, no strikingly increased levels of lysosomes were detected inside the cells, which support the biocompatibility of both tested silica materials. It was also apparent that the particles keep an intact pore structure within the cells.

In conclusion, our data show that both size and concentration correlate with effect, where the smaller silica particles and lower concentrations in general affected MDDC to a minor degree compared to the larger particles and higher concentrations, both in terms of viability, uptake, and immune regulatory markers, which was seen by the induction of IL-12p70 and CD86 and a decreased expression of CD80 and CD40. The results show that the cellular uptake of both particles is mediated by an active process but where the intracellular localization seems to differ. All together, our data suggest different applications for the tested mesoporous silica material due to the size, where AMS-8 has promising features to serve as an immune-stimulant/regulant with possible T-cell modulatory properties, while AMS-6 is rather a potential candidate for a more neutral drug delivery system. Similar size dependent immunogencity has been reported before, where the vaccine efficiency of polystyrene was critically dependent on the size of the particles.[29] Taken together with the relatively low-toxicity profiles on MDDC and the mesoporous structures of both silica particles, the particles provide a promising approach worth further development into drug/vaccine delivery systems.

Acknowledgment. We wish to thank Osamu Terasaki (Stockholm University, Sweden) for access to his TEM facility as well as many helpful discussions and Kjell Hultenby (Clinical Research Center, Karolinska University Hospital Huddinge, Sweden) for his help with TEM analysis of MDDC. We thank Daniel Olsson at the Department of Medical Informatics and Educational Development, Medical Statistics Unit, Karolinska Institutet, Stockholm, for assistance with statistical analysis. We also thank Bengt Fadeel and Erika Witasp (Institute of Environmental Medicine, Karolinska Institutet) for fruitful discussions and Bengt Fadeel for comments on the manuscript. This study was supported by grants from the Swedish Research Council for Working Life and Social Research, the Swedish Research Council, and by an unrestricted grant from TERUMO EUROPE N.V. and Karolinska Institutet.

Supporting Information Available: Detailed accounts of the experimental procedures for the synthesis of mesoporous particles of AMS-6 and AMS-8 and for the cellular experiments are included. Two movie files (.wmv) corresponding to z-scan confocal microscopy images of MDDC co-cultured with AMS-6 and AMS-8 at 4 °C are also included. The material is available free of charge via the Internet at http://pubs.acs.org.

References

(1) Kresge, C. T.; Leonowicz, M. E.; Roth, W. J.; Vartuli, J. C.; Beck, J. S. *Nature* **1992**, *359*, 710−2.
(2) Schüth, F.; Schmidt, W. *Adv. Mater.* **2002**, *14*, 629−38.
(3) Schüth, F.; Taguchi, A. *Microporous Mesoporous Mater.* **2004**, *77*, 1−45.
(4) Vallet-Regi, M. *Chem.—Eur. J.* **2006**, *12*, 5934−43.
(5) Vallet-Regi, M.; Ramila, A.; del Real, R. P.; Perez-Pariente, *J. Chem. Mater.* **2001**, *13*, 308−11.
(6) Yiu, H. H. P.; Wright, P. A. *J. Mater. Chem.* **2005**, *15*, 3690−700.
(7) Radu, D. R.; Lai, C.-Y.; Jeftinija, K.; Rowe, E. W.; Jeftinija, S.; Lin, V. S.-Y. *J. Am. Chem. Soc.* **2004**, *126*, 13216−7.
(8) Clupper, D. C.; Mecholsky, J. J., Jr.; LaTorre, G. P.; Greenspan, D. C. *Biomaterials* **2002**, *23*, 2599−06.
(9) Pereira, M. M.; Jones, J. R.; Hench, L. L. *Adv. Appl. Ceram.* **2005**, *104*, 35−42.
(10) Chithrani, B. D.; Ghazani, A. A.; Chan, W. C. W. *Nano Lett.* **2006**, *6*, 662−8.
(11) Banchereau, J.; Steinman, R. M. *Nature* **1998**, *392*, 245−52.
(12) Yamazaki, S.; Inaba, K.; Tarbell, K. V.; Steinman, R. M. *Immunol. Rev.* **2006**, *212*, 314−29.
(13) Larché, M.; Akdis, C. A.; Valenta, R. *Nat. Rev. Immunol.* **2006**, *6*, 761−71.
(14) Lohr, J.; Knoechel, B.; Abbas, A. K. *Immunol. Rev.* **2006**, *212*, 149−62.
(15) Garcia-Bennett, A. E.; Lund, K.; Terasaki, O. *Angew. Chem., Int. Ed.* **2006**, *45*, 2434−8.
(16) Garcia-Bennett, A. E.; Miyasaka, K.; Che, S.; Terasaki, O. *Chem. Mater.* **2004**, *16*, 3597−605.
(17) Garcia-Bennett, A. E.; Kupferschmidt, N.; Sakamoto, Y.; Che, S.; Terasaki, O. *Angew. Chem., Int. Ed.* **2005**, *44*, 5451−6.
(18) Brunauer, S.; Emmett, P. H.; Teller, E. *J. Am. Chem. Soc.* **1938**, *60*, 309−19.

(19) Vallhov, H.; Qin, J.; Johansson, S. M.; Ahlborg, N.; Muhammed, M. A.; Scheynius, A.; Gabrielsson, S. *Nano Lett.* **2006**, *6*, 1682−6.
(20) Romani, N.; Gruner, S.; Brang, D.; Kämpgen, E.; Lenz, A.; Trockenbacher, B.; Konwalinka, G.; Fritsch, P. O.; Steinman, R. M.; Schuler, G. *J. Exp. Med.* **1994**, *180*, 83−93.
(21) Wang, Y.; Li, X.; Wang, L.; Ding, P.; Zhang, Y.; Han, W.; Ma, D. *J. Cell Sci.* **2004**, *117*, 1525−32.
(22) Mishra, D. P.; Dhali, A. *Prostaglandins* **2007**, *83*, 75−88.
(23) Buentke, E.; Heffler, L. C.; Wallin, R. P. A.; Löfman, C.; Ljunggren, H. G.; Scheynius, A. *Clin. Exp. Allergy* **2001**, *31*, 1583−93.
(24) Gao, D.; Mondal, T. K.; Lawrence, D. A. *Toxicol. Appl. Pharmacol.*, in press.
(25) Bhatia, S.; Edidin, M.; Almo, S. C.; Nathenson, S. G. *Immunol. Lett.* **2006**, *104*, 70−5.
(26) Iijima, N.; Yanagawa, Y.; Iwabuchi, K.; Onoé, K. *Immunology* **2003**, *110*, 197−205.
(27) Chen, M.; von Mikecz, A. *Exp. Cell. Res.* **2005**, *305*, 51−62.
(28) Slowing, I. I.; Trewyn, B. G.; Lin, V. S.-Y. *J. Am. Chem. Soc.* **2007**, *129*, 8845−9.
(29) Minigo, G.; Scholzen, A.; Tang, C. K.; Hanley, J. C.; Kalkanidis, M.; Pietersz, G. A.; Apostolopoulos, V.; Plebanski, M. *Vaccine* **2007**, *25*, 1316−27.

NL0714785